Scaled Opposite Spin Second Order Møller−Plesset Theory with Improved Physical Description of Long-Range Dispersion Interactions

Rohini C. Lochan, Yousung Jung, and Martin Head-Gordon*

Department of Chemistry, University of California, Berkeley, and Chemical Sciences Division, Lawrence Berkeley National Laboratory, Berkeley, California 94720

Received: March 19, 2005; In Final Form: June 10, 2005

Separate scaling of the same-spin and opposite spin contributions to the second-order Møller−Plesset energy can yield statistically improved performance for a variety of chemical problems. If only the opposite spin contribution is scaled, it is also possible to reduce the computational complexity from fifth order to fourth order in system size, with very little degradation of the results. However neither of these scaled MP2 energies recovers the full MP2 result for the dispersion energy of nonoverlapping systems. This deficiency is addressed in this work by using a distance-dependent scaling of the opposite spin correlation energy. The resulting method is compared against the previously proposed scaled MP2 methods on a range of problems involving both short and long-range interactions.

I. Introduction

Møller−Plesset perturbation theory[1] is a popular electronic structure theory that can approximately evaluate the correlation energy of molecules. In particular, second-order Møller−Plesset perturbation theory (MP2) offers the simplest and least expensive wave function based treatment of electron correlation beyond the Hartree−Fock (HF) approximation.[2] MP2 has certain advantages over the widely used density functional theory (DFT)[3] as it provides a fairly accurate description of the important long-range dispersion interactions,[4] which present-day density functionals completely neglect.[5] However, MP2 is still plagued by several problems like high computational cost, the need for large basis sets to obtain fairly accurate results[6] and poor description of open shell systems.[7]

In recent years, there has been considerable focus on addressing the high computational cost of MP2 whose bottleneck is the fifth order scaling four-index integral transformation.[8] This led to the development of several efficient approaches that attempt to work around this bottleneck. For example there are local MP2 methods that define a local correlation space and discard some or all of the nonlocal terms to obtain large reduction in the computational effort by either using localized orbitals[9−11] or employing atomic truncations.[12] Then there is the cutoff based formulation of MP2 in the atomic orbital basis that has shown linear scaling behavior for one-dimensional systems with small basis sets.[13,14] The "resolution-of-the-identity" (RI)-MP2 method is an efficient and popular approach that uses auxiliary basis expansions to avoid the computation of the four-index integral transformation and hence achieve significant speed-ups.[15,16]

It is certainly desirable to explore enhancements to the basic MP2 method that permit increased accuracy as well as improved computational performance. Following this theme, recently, the idea of using separate scaling of the same-spin (SS) and opposite-spin (OS) correlation energies was proposed by Grimme[17] and led to significant statistical improvements over MP2 results for a range of properties.[18−20] This approach is called "spin-component scaled" (SCS) MP2. In MP2 theory, the correlation energy can be written as

$$E_{\mathrm{MP2}} = E_{\mathrm{OS}} + E_{\mathrm{SS}} \tag{1}$$

E_{OS} and E_{SS} are the contributions of the opposite-spin ($\alpha\beta$) and same-spin ($\alpha\alpha$ and $\beta\beta$) components to the total MP2 correlation energy. The SCS-MP2 energy is defined as

$$E_{\mathrm{MP2}} = c_{\mathrm{OS}}E_{\mathrm{OS}} + c_{\mathrm{SS}}E_{\mathrm{SS}} \tag{2}$$

where Grimme's recommended scaling factors are $c_{\mathrm{OS}} = 1.2$ and $c_{\mathrm{SS}} = 0.3$.

Following this development, we recently suggested an even simpler variant of SCS-MP2 called "scaled opposite-spin" (SOS) MP2.[21] Motivated by the large damping of the SS part in SCS-MP2 and also noticing that the evaluation of the SS component energy leads to most of the observed computational complexities, we completely neglect the SS component of the correlation energy and scale only the OS part. The proposed scaling factors in eq 2 are now $c_{\mathrm{OS}} = 1.3$ and $c_{\mathrm{SS}} = 0$. This approach was shown to have a 2-fold advantage in keeping with the theme of "improved accuracy and reduced scaling". First, with only a single parameter, we were able to largely retain the statistical improvements obtained by the SCS-MP2 approach over a range of properties and second, we showed without using cutoffs that SOS-MP2 energy can be evaluated with a fourth order scaling algorithm using a combination of auxiliary basis functions and a Laplace transform in contrast with the conventional fifth order scaling MP2 method.

However, one undesirable feature of both the SCS-MP2 and SOS-MP2 methods, apart from their empirical parameter(s), is the incorrect physical description of the long-range correlation between two nonoverlapping systems. In this long-range regime, if we assume that the two systems of interest are closed shell, the SS and OS components to the inter-system correlation energy should be exactly equal as can be readily verified. Therefore, the appropriate scaling factor for opposite correlation alone should approach 2. The scaling factors of SCS-MP2 and SOS-

* To whom correspondence should be addressed. E-mail: mhg@cchem.berkeley.edu.

10.1021/jp0514426 CCC: $30.25
Published on Web 08/04/2005

MP2 are around 1.5 and 1.3 respectively at this limit and thus tend to significantly underestimate the MP2 correlation energy. Hence, these theories are not going to be very accurate for systems where long-range interactions are of critical importance. This assumes that MP2 theory itself is accurate for long-range dispersion interactions, which is usually (but not always) true.[22]

The purpose of this paper is to suggest an alternative scaled opposite-spin technique that can get the long-range description correct by construction while still retaining the desirable features of SOS-MP2 at almost no extra cost. The idea is to determine and use a correcting factor that depends on the inter-electronic distance rather than a simple constant scaling factor. With this intent, we define a long-range operator as follows:

$$\hat{L}_\omega(\mathbf{r}) = \frac{\mathrm{erf}(\omega \mathbf{r})}{\mathbf{r}} \tag{3}$$

This operator was previously used in the context of separation of the Coulomb operator ($1/\mathbf{r}$) into a nonsingular but slowly and smoothly decaying long-range piece, $\hat{L}_\omega(\mathbf{r})$ and a singular but rapidly decaying short-range part, $\hat{S}_\omega(\mathbf{r}) = \mathrm{erfc}(\omega\mathbf{r})/\mathbf{r}$ in order to gain computational efficiency.[23,24] For our purposes, we would like to take advantage of the behavior of this long-range operator that approaches $1/\mathbf{r}$ as $\mathbf{r} \rightarrow \infty$ and define a new "modified" two-electron operator, $\hat{g}_\omega(\mathbf{r})$,

$$\hat{g}_\omega(\mathbf{r}) = \hat{g}(\mathbf{r}) + c_{MOS}\hat{L}_\omega(\mathbf{r}) \tag{4}$$

with $\hat{g}(r) = 1/\mathbf{r}$, leading to a new set of "modified" integrals ($\tilde{I}_\omega$),

$$\tilde{I}_{ia}^{jb}(\omega) = \int d\mathbf{r} \int d\mathbf{r}' \phi_i(\mathbf{r})\phi_a(\mathbf{r})\hat{g}_\omega(\mathbf{r}-\mathbf{r}')\phi_j(\mathbf{r}')\phi_b(\mathbf{r}') \tag{5}$$

so that the "modified" opposite-spin (MOS)-MP2 energy is now given by

$$E_{\mathrm{MP2}}^{\mathrm{MOS}}(\omega) = -\sum_{ia}^{\alpha}\sum_{jb}^{\beta}\frac{\tilde{I}_{ia}^{jb}(\omega)\tilde{I}_{ia}^{jb}(\omega)}{\Delta_{ia}^{jb}} \tag{6}$$

The energy denominator is defined in terms of the canonical orbital energies of the occupied levels i, j and virtual levels a, b as $\Delta_{ia}^{jb} = (\epsilon_a - \epsilon_i) + (\epsilon_b - \epsilon_j)$. The variable c_{MOS} ($= \sqrt{2} - 1$) in eq 4 is easily fixed by the requirement that $E_{\mathrm{MP2}}^{\mathrm{MOS}} \rightarrow 2E_{\mathrm{MP2}}^{\mathrm{OS}}$ as $\mathbf{r} \rightarrow \infty$. MOS-MP2 is dependent on a single parameter ω, an optimal value for which can be determined empirically by performing chemical tests. This is explored in detail in section II.

In this paper, we first assess and compare MOS-MP2, in section II, against conventional MP2, SCS-MP2, and SOS-MP2 by performing a range of chemical tests similar to those in Jung et al..[21] We have further included some examples of rare-gas dimers and hydrogen-bonded molecules where a correct description of long-range correlation is important. In section III, we present the "modified" fourth order scaling algorithm to efficiently compute the MOS-MP2 energy, without exploiting localization. Our approach uses auxiliary basis functions, together with a Laplace approach to eliminate energy denominators and is very similar to the recently suggested SOS-MP2 algorithm. Section IV explores a chemical application of MOS-MP2 that demonstrates the usefulness and computational effectiveness of this method. Finally, we present some conclusions.

II. Chemical Tests

All calculations reported in this paper were performed using a developmental version of the Q-CHEM program,[25] where our standard MP2 program[26] was modified to evaluate the SCS-MP2, SOS-MP2, and MOS-MP2 energy. The objective of this section is to evaluate MOS-MP2's performance and compare against the performance of conventional MP2, SCS-MP2, and SOS-MP2 and high level correlation methods like QCISD and QCISD(T)[27] using the Dunning cc-pVTZ basis set.[28] We would also like to choose an optimal value for the parameter ω based on these chemical tests. We have used the same database of 41 reaction energies and 30 barrier heights considered in our recent SOS-MP2 paper,[21] which includes further technical details. We have replaced the 77 atomization energies considered in ref 21 with the atomization energies calculated for the entire G2 test set[29,30] of 148 neutral molecules (MP2/6-31G* optimized geometries).

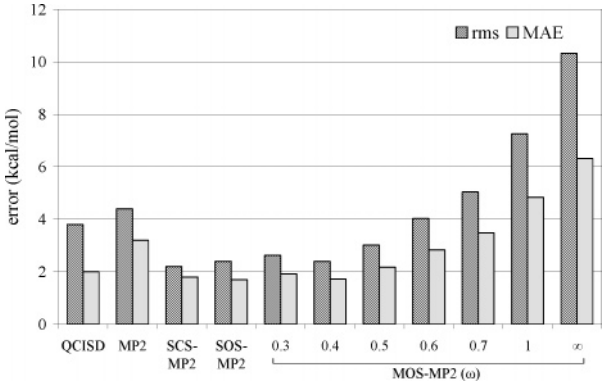

Figure 1. Root mean squared and mean absolute errors of the 41 reaction energies[21] calculated relative to QCISD(T) with cc-pVTZ basis.

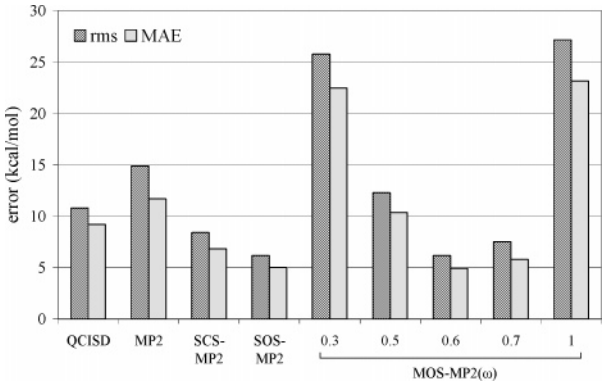

Figure 2. Root mean squared and mean absolute errors of the 148 atomization energies of G2-neutral test set calculated relative to QCISD(T) with cc-pVTZ basis.

A. Reaction Energies, Atomization Energies, and Barrier Heights. We have evaluated the reaction energies, atomization energies, and barrier heights via MOSMP2 over a range of ω values. Figures 1−3 show the statistics of the rms error and mean absolute error (MAE) generated by the various methods with QCISD(T) energies taken as the reference for each property, respectively. Looking at the reaction energy data (Figure 1), we infer that MOS-MP2 ($\omega = 0.3-0.6$) performs better than MP2. The least rms error is obtained by MOS-MP2 ($\omega = 0.4$) and this is almost as good as SCS-MP2 and slightly better than SOS-MP2. For atomization energies, MOS-MP2 ($\omega = 0.6-0.7$) shows a great improvement (a reduction of $\sim$ 8−9 kcal/mol) over MP2 rms error. In particular, MOS-MP2 ($\omega = 0.6$) is more favorable than SCS-MP2 and very similar to performance of SOS-MP2. Estimation of barrier heights proved to be difficult for both SOS-MP2 and SCS-MP2 relative to MP2 but by letting ω values vary between 0.6 and 2, MOS-MP2 seems to overcome this problem! For instance, the rms error of

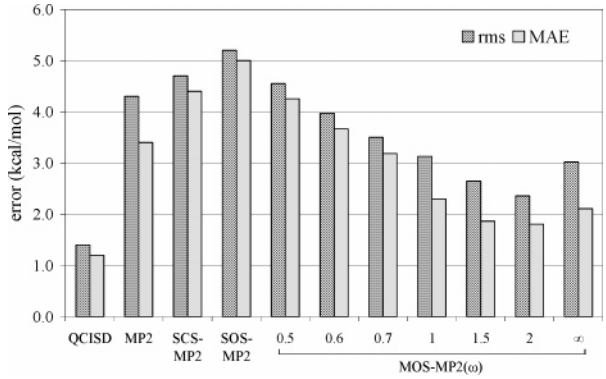

Figure 3. Root mean squared and mean absolute errors of the 30 barrier heights[21] calculated relative to QCISD(T) with cc-pVTZ basis.

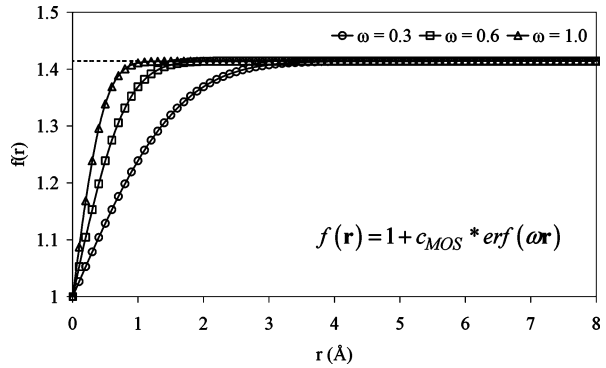

Figure 4. Variation of the opposite spin scaling factor with inter-electronic distance.

MOS-MP2 ($\omega = 1.5$) is almost 2 kcal/mol lower than that of conventional MP2.

The above observations suggest that the modification of the simple SOS-MP2 idea, not only retains the advantages obtained in SCS-MP2 and SOS-MP2, but also improves upon the problems encountered in case of barrier heights. In fact, one can really tune the ω value used in MOS-MP2 to obtain the best results for a particular property (similar in spirit to the development of density functionals that are optimized for "kinetics" via fitting to barrier heights[31]). This possibility will not, however, be explored further here. Instead we seek a single value most suitable for general-purpose use. On the basis of the discussion above, MOS-MP2 ($\omega = 0.6$) seems to be a value that consistently performs better than MP2 across the entire database. Hereafter, we will retain $\omega = 0.6$ as the default parameter value for the remainder of the paper unless specified. It is worthwhile to mention here that the parameter ω determines the distance at which the asymptotic limit of $\hat{g}_\omega(\mathbf{r}) \rightarrow \sqrt{2}\cdot\hat{g}(\mathbf{r})$ (eq 4) is approximately reached. This can be easily measured by plotting $f(\mathbf{r})(= 1 + c_{\mathrm{MOS}} \times \mathrm{erf}(\omega\mathbf{r}))$ vs $\mathbf{r}$. Figure 4 shows that the limit is reached at longer distances for smaller ω values. For example, with $\omega = 0.6$ au this limit is reached around $\mathbf{r} \sim 2$ Å. In other words, the contribution of the modified integrals in eq 5 to the MOS-MP2 energy (eq 6) is scaled by a factor of 2 only when the corresponding inter-electronic distance is greater than 2 Å. This ensures that contributions from the electrons correlating strongly over a short range ($\mathbf{r} < 2$ Å) are scaled by a factor smaller than 2 in keeping with the idea of SCS- and SOS-MP2.

B. Interactions of Weakly Bound Dimers. Since the MOS-MP2 method is designed to recover the MP2 result for the dispersion energy of nonoverlapping molecules, it is particularly relevant to investigate its performance for weak interactions like rare-gas dimers and a few hydrogen-bonded molecules. Constrained geometry optimization (MP2/6-31G*) was carried out for the water-dimer at 8 different O−O separations (between 2.4 and 5.0 Å) and for the rare-gas dimers, about 20 points between 3 and 9 Å were considered. The interaction energies were then computed through single-point calculations at the MP2, SCS-MP2, SOS-MP2, and MOS-MP2 levels using the augmented correlation-consistent polarized valence *X*-ζ (aug-cc-pV*X*Z, X = T, Q) basis sets of Dunning.[28,32] Standard counterpoise corrections (CP) were applied to the reported potential energy curves to account for basis set superposition errors (BSSE). Extrapolated results at the complete basis set limit (CBS) was estimated by applying a simple two-point extrapolation scheme,[33] where the error in the aug-cc-pV*X*Z basis is given by

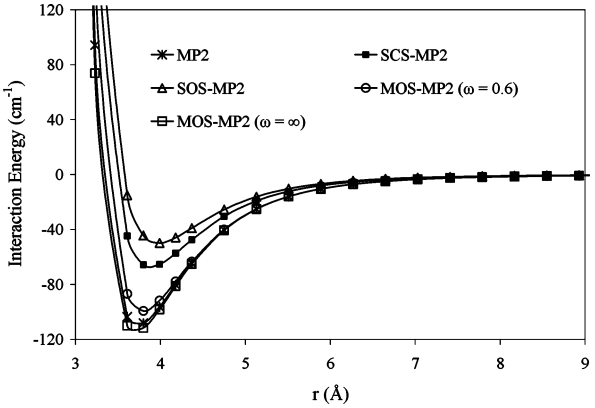

Figure 5. Counterpoise corrected potential energy curve of argon dimer at complete basis limit.

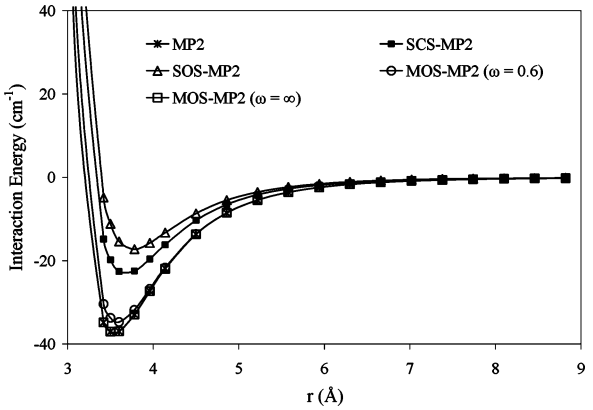

Figure 6. Counterpoise corrected potential energy curve of argon−neon dimer at complete basis limit.

$$\Delta E_X \propto X^{-3} \tag{7}$$

Figures 5−7 show the CP corrected interaction potential curves for Ar−Ar, Ne−Ar, and H_2O-H_2O dimers at CBS for the method MP2 and its variants SCS-MP2 and SOS-MP2. Also shown are the MOS-MP2 curves for the cases of $\omega = 0.6, \infty$. Following the observations made in section I, it is apparent that SOS-MP2 and SCS-MP2 curves underestimate the binding energy especially close to equilibrium distance and this underestimation is visible until almost 6 Å separation for the rare-gas dimer molecules, Ar−Ar and Ne−Ar. MOS-MP2 ($\omega = 0.6$) on the other hand is in close agreement with the MP2 curve in case of the rare-gas dimers. For instance, if we consider the Ar−Ar dimer close to equilibrium distance (refer Table 1), the SOS-MP2 interaction energy is underestimated by ∼60%, while SCS-MP2 is ∼40% too low relative to MP2. By contrast MOS-

TABLE 1: Comparison of the Interaction Energy of Ar−Ar, Ne−Ar, and Water Dimer at a Specific Geometry Close to the Minimum in the Respective Potential Energy Curves

	basis	MP2	SCS-MP2	SOS-MP2	MOS-MP2[a]	CCSD(T)
Ar−Ar[b]						
without CP[c]	aug-cc-pVTZ	−110.68	−74.93	−57.06	−102.86	
	aug-cc-pVQZ	−112.23	−73.33	−53.88	−103.86	
with CP[c]	aug-cc-pVTZ	−84.34	−45.93	−26.72	−77.21	−69.30[d]
	aug-cc-pVQZ	−97.60	−56.80	−36.40	−89.48	−82.97[d]
	extrapolated	−108.18	−65.64	−44.37	−99.34	−96.86[e]
						−99.54[f]
Ne−Ar[b]						
without CP[c]	aug-cc-pVTZ	−44.83	−31.63	−25.03	−41.78	
	aug-cc-pVQZ	−43.95	−29.07	−21.63	−40.64	
with CP[c]	aug-cc-pVTZ	−24.83	−9.73	−2.19	−22.47	−28.64[d]
	aug-cc-pVQZ	−31.78	−15.45	−7.28	−28.90	−37.28[d]
	extrapolated	−37.01	−19.78	−11.16	−33.74	−45.17[e]
						−46.98[f]
H2O−H2O[g]						
without CP[c]	aug-cc-pVTZ	−5.04	−4.72	−4.56	−4.69	−5.15[h]
	aug-cc-pVQZ	−4.94	−4.61	−4.44	−4.59	−5.05[h]
with CP[c]	aug-cc-pVTZ	−4.63	−4.26	−4.08	−4.30	−4.68[h]
	aug-cc-pVQZ	−4.74	−4.38	−4.20	−4.40	−4.86[h]
	extrapolated	−4.81	−4.45	−4.27	−4.46	−4.96[h]
						−4.85[i]

[a] $w = 0.6$. [b] Energies in cm^{-1}; $r_{Ar-Ar} = 3.80$ Å; $r_{Ne-Ar} = 3.50$ Å. [c] CP: counterpoise correction. [d] Data taken from Cybulski et al.[34] [e] CCSD(T) interaction energy computed with aug-cc-pV5Z supplemented with bond functions (3s3p2d2f1 g), taken from Cybulski et al.[34] [f] Values from experimentally derived potential energy surface from Ogilvie et al.[44] ($r_{Ar-Ar} = 3.76$ Å, $r_{Ne-Ar} = 3.48$ Å). [g] Energies in kcal/mol; r_{O-O} in water dimer = 3.00 Å. [h] Data taken from Halkier et al.[36] Geometry optimized at CCSD(T)/aug-cc-pVTZ level; r_{O-O} in water dimer = 2.90 Å. [i] Estimated binding energy from spectroscopic studies of Goldman et al.;[37] equilibrium r_{O-O} in water dimer = 2.95 Å.

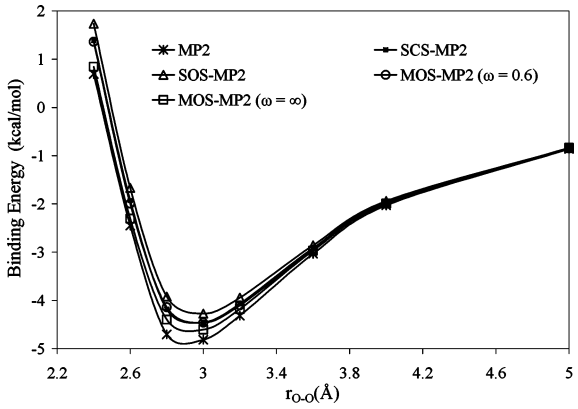

Figure 7. Counterpoise corrected potential energy curve of water dimer at complete basis limit.

MP2 ($\omega = 0.6$) is only off by ~ 9%. A similar trend is observed for the Ne−Ar dimer. This underestimation can prove to be a boon for the scaled MP2 theories if conventional MP2 generally tends to overestimate the interaction energies. However, comparing the regular MP2 results with those obtained from higher-level correlation methods like CCSD(T) at CBS limit (last column in Table 1, data collated from Cybulski et al.[34]) reflects that MP2 overestimates the interaction energy in case of Ar−Ar dimer and underestimates in case of Ne−Ar dimer. So it is possible that the gross underestimation of SCS-MP2 and SOS-MP2 results could deteriorate the quality of MP2 energies, especially for nonoverlapping systems like Ne−Ar dimer. MOS-MP2 on the other hand is able to predict MP2-like results.

For the water dimer, the underestimation of binding energy by SCS-MP2 (~ 0.4 kcal/mol) and SOS-MP2 (~0.5 kcal/mol) relative to MP2 still holds true. However, the MOS-MP2 ($\omega = 0.6$) curve lies almost on top of the SCS-MP2 curve, unlike the improvements seen in the rare-gas dimers. At first glance, one might think that the reason for this odd behavior could be an improper choice of ω value. So, if we consider the extreme case of MOS-MP2 with $\omega = \infty$, where the binding energy calculated would be twice that of the binding energy contribution of opposite-spin component of the conventional MP2 method, we expect to overestimate the MP2 binding energy at short and intermediate distances. The curves for MOS-MP2 ($\omega = \infty$) in Figures 5−7, however, do not seem to follow this expectation. This curve seems to coincide with the regular MP2 curve in case of Ar−Ar dimer and lies slightly above the MP2 curve for Ne−Ar dimer and water dimer. To understand this behavior, we have tabulated the contributions of the opposite-spin (OS) and same-spin components (SS) of the total MP2 correlation energy toward the binding energy in Table 2 for Ar−Ar dimer, Ne−Ar dimer, and water dimer at various dimer distances using the cc-pVTZ basis. We have also included some more hydrogen-bonded molecules like CH_3OH-H_2O, HCN−HF, HF−HF, NH_3-H_2O, and NH_3-NH_3 at their equilibrium geometry, obtained from MP2/6-31G* geometry optimization. We have also included the coupled-cluster singles and doubles (CCSD)[35] correlation energy breakdown into SS and OS components for comparison purposes. The CCSD correlation energies are smaller in magnitude compared to MP2 correlation energies due the well-known fact that MP2 tends to overestimate the doubles contribution while CCSD partly includes the effect of quadruple excitations through "disconnected" T_2^2 contributions. Looking at Table 2, the first observation is that for the rare-gas dimers, the contributions of the SS and OS toward the MP2 binding energy are very similar at distances close to and around the equilibrium distance, with and without CP correction. In other words, the MP2 binding energy is roughly two times that of the OS contribution. A similar trend is also observed with the CCSD energies. This explains why the MOS-MP2 ($\omega = \infty$) almost coincided with the regular MP2 curve and emphasizes that exclusion (SOS-MP2) or damping (SCS-MP2) of the SS component results in underestimation of the total binding energy.

In case of the hydrogen-bonded molecules, the non-CP corrected binding energies are very similar, within 0.2 kcal/mol for both SS and OS close to the equilibrium dimer separation, except for the dimers where HF is involved. However, with the inclusion of CP correction for BSSE, the SS component seems to contribute ~0.4−0.9 kcal/mol more

TABLE 2: Breakdown of Contribution of MP2 Total Correlation Energy (ΔE_{MP2}) toward Binding Energy

		ΔE_{MP2}[b]				ΔE_{CCSD}[c]			
		no CP[d]		CP[d]		no CP[d]		CP[d]	
molecule	r[a]	ΔE_{OS}[e]	ΔE_{SS}[e]	ΔE_{OS}[e]	ΔE_{SS}[e]	ΔE_{OS}[e]	ΔE_{SS}[e]	ΔE_{OS}[e]	ΔE_{SS}[e]
Ar−Ar[f]	2.85	−1709.80	−1647.75	−1432.10	−1540.87	−1155.96	−1353.61	−896.68	−1256.32
	3.80	−283.31	−266.86	−231.91	−243.36	−193.76	−214.93	−147.77	−196.45
	4.75	−60.49	−57.94	−54.83	−55.29	−39.56	−44.92	−35.31	−43.35
	5.89	−14.34	−14.31	−14.27	−14.27	−9.12	−11.01	−9.07	−10.99
Ar−Ne[f]	3.06	−240.63	−238.35	−95.90	−165.15	−176.99	−214.46	−53.95	−161.57
	3.60	−108.13	−88.56	−52.05	−59.18	−84.35	−74.98	−39.46	−55.67
	4.86	−9.41	−9.23	−8.97	−9.00	−7.27	−8.16	−6.95	−8.02
	5.58	−3.84	−3.83	−3.83	−3.83	−2.95	−3.40	−2.95	−3.39
	6.66	−1.29	−1.29	−1.29	−1.29	−0.99	−1.14	−0.99	−1.14
H_2O-H_2O[g]	2.40	−2.40	−2.45	−0.99	−1.76	−1.67	−2.38	−0.58	−1.91
	2.60	−1.89	−1.91	−0.71	−1.30	−1.29	−1.81	−0.39	−1.40
	2.80	−1.38	−1.70	−0.47	−1.32	−0.70	−1.65	0.03	−1.41
	3.00	−1.07	−1.23	−0.35	−0.92	−0.58	−1.17	−0.01	−0.97
	3.20	−0.81	−0.89	−0.26	−0.63	−0.46	−0.81	−0.03	−0.65
	3.60	−0.45	−0.47	−0.13	−0.30	−0.26	−0.39	−0.02	−0.30
	4.00	−0.27	−0.26	−0.05	−0.15	−0.15	−0.20	0.00	−0.14
CH_3OH-H_2O[h]		−1.82	−1.99	−0.72	−1.51	−1.07	−1.87	−0.15	−1.56
HCN−HF[h]		−0.70	−1.13	0.00	−0.94	−0.09	−1.12	0.54	−1.01
HF−HF[h]		−0.07	−0.71	0.39	−0.56	−0.01	−0.80	0.40	−0.70
NH_3-H_2O[h]		−1.78	−1.99	−0.89	−1.65	−0.91	−1.84	−0.22	−1.64
NH_3-NH_3[h]		−1.42	−1.45	−0.85	−1.21	−0.86	−1.33	−0.42	−1.20

[a] Dimer separation (Å). [b] $\Delta E_{Binding} = \Delta E_{Hartree-Fock} + \Delta E_{MP2}$. [c] $\Delta E_{Binding} = \Delta E_{Hartree-Fock} + \Delta E_{CCSD}$. [d] CP: counterpoise corrected interaction energy. [e] $\Delta E_{MP2} = \Delta E_{Same\ Spin\ (SS)} + \Delta E_{Opposite\ Spin\ (OS)}$; similarly for CCSD. [f] cc-pVTZ basis; energies in μE_h. [g] cc-pVTZ basis; energies in mE_h. [h] cc-pVTZ basis; energies in mE_h for MP2/6-31G* optimized structures.

than OS component toward the binding energy. This trend is observed for both non-CP and CP corrected breakdown of the CCSD correlation energy around the equilibrium dimer separation and the difference between the SS and OS component is even greater, ∼0.5−1.0 and ∼0.8−1.4 kcal/mol, respectively. This means that even in the extreme case of MOS-MP2 ($\omega = \infty$), twice the OS component's contribution of the MP2 binding energy will never be able to compensate for the missing SS component contribution that is greater in magnitude. This accounts for the odd behavior of the MOS-MP2 curves in Figures 5−7.

It is also interesting to note that for the water dimer, the CP corrected binding energies at CBS limit predicted by regular MP2 and CCSD(T)[36] are within ∼0.1 kcal/mol agreement with the experiment value[37] (see Table 1). MOS-MP2, however, underestimates the interaction energy by ∼0.4 kcal/mol relative to experiment but the good news is that it improves the SOS-MP2 results by ∼0.2 kcal/mol.

III. Fourth Order Algorithm Using Auxiliary Basis Expansion and Laplace Transformation

The evaluation of MOS-MP2 energy can also be performed without any fifth order step, unlike conventional MP2 theory, similar to the SOS-MP2[21] algorithm but with certain modifications. Following Almlöf,[38] the energy denominator in eq 6 can be eliminated via the Laplace transformation $1/x = \int_0^\infty \exp(-xt)\, dt$ and the integration over t can be replaced by a discrete quadrature (involving Q points) to get

$$E_{MP2}^{MOS}(\omega) = -\sum_{q}^{Q}\sum_{ia}^{\alpha}\sum_{jb}^{\beta}\tilde{I}_{ia}^{jb}(\omega;q)\tilde{I}_{ia}^{jb}(\omega;q) \tag{8}$$

$$\tilde{I}_{ia}^{jb}(\omega;q) = \tilde{I}_{ia}^{jb}(\omega) w_q^{1/2} \exp\left(-\frac{1}{2}\Delta_{ia}{}^{jb} t_q\right) \tag{9}$$

We now introduce an auxiliary basis for the evaluation of the two-electron integrals, which is crucial for eliminating the fifth order step in conventional MP2 and RI-MP2.[15,16] Denoting the auxiliary functions by K, L, ..., and recognizing the fact that we can use any metric to fit the two-electron integrals irrespective of the two-electron operator,[39,40] the "modified" operator from eq 4 is used as the fitting metric to get $\tilde{I}_{ia}^{jb}(\omega;q)$in terms of two- and three- center integrals as follows,

$$\tilde{I}_{ia}^{jb}(\omega;q) = \sum_{K}\tilde{B}_{ia}^{K}(\omega;q)\tilde{B}_{jb}^{K}(\omega;q) \tag{10}$$

$$\tilde{B}_{ia}^{K}(\omega;q) = \sum_{M}\sum_{\mu\nu} w_q^{1/4}\{C_{\nu a}\exp(-\epsilon_a t_q/2)[C_{\mu i}\exp(\epsilon_i t_q/2)(\mu\nu|M)_\omega]\} (\tilde{V}_\omega^{MK})^{-1/2} \tag{11}$$

$$\tilde{V}_\omega^{MK} = (M|K)_\omega \tag{12}$$

The use of the two-electron operator $\hat{g}_\omega(\mathbf{r})$ from eq 4 (denoted by subscript ω) in the above equations will yield fitted $\tilde{I}_{ia}^{jb}(\omega;q)$ with second-order error as the same metric is used in both integral evaluation and fitting.[41] We can now use eq 10 to rewrite eq 8 as

$$E_{MP2}^{MOS} = -\sum_{q}^{Q}\sum_{ia}^{\alpha}\sum_{jb}^{\beta}\sum_{KL}\tilde{B}_{ia}^{K}(\omega;q)\tilde{B}_{jb}^{K}(\omega;q)\tilde{B}_{ia}^{L}(\omega;q)\tilde{B}_{jb}^{L}(\omega;q) = -\sum_{q}^{Q}\sum_{KL}\tilde{X}_{KL}^{\alpha}(\omega;q)\tilde{X}_{KL}^{\beta}(\omega;q) \tag{13}$$

This working expression is now directly in terms of the auxiliary basis, very similar to the corresponding expression in the SOS-MP2 formalism,[21] but with a modified definition for $\mathbf{X}$

$$\tilde{X}_{KL}^{\alpha}(\omega;q) = \sum_{ia}^{\alpha}\tilde{B}_{ia}^{K}(\omega;q)\tilde{B}_{ia}^{L}(\omega;q) \tag{14}$$

The implementation and the computational cost analysis of the above are very similar to the discussion in our recent SOS-

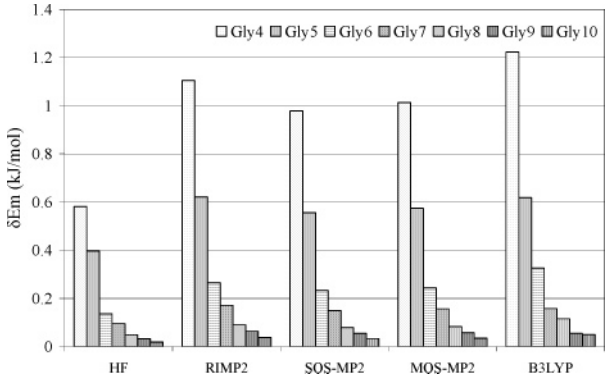

Figure 8. Decay of stabilization energy of Gly_m computed at various levels of theory. The cc-pVTZ basis set was used for HF and B3LYP calculations. The extrapolated results at CBS are shown for RI-MP2, SOS-MP2, and MOS-MP2.

MP2 paper.[21] The only extra cost arises from the evaluation of the long-range correction term in the two and three-center integrals, $\tilde{V}_\omega$ and $(\mu\nu|M)_\omega$, which are both second-order steps. The rest of the algorithm follows the same exact cost analysis as SOS-MP2. The formation of the $\tilde{\mathbf{X}}$ matrix in eq 14 continues to be the dominating fourth order step. We thus expect the cost of computing MOS-MP2 and SOS-MP2 energies to be almost similar.

IV. Chemical Application: Study of Long-Range Stabilization Energies in β-Sheet Oligoglycines

Horvath et al.[42] recently studied the long-range interactions in the β-sheet structure of oligoglycines (Gly_m; $m = 2-10$) using DFT (B3LYP) methodology. They found that long-range interactions operating through hydrogen bonds and dipole−dipole interactions leads to a cooperative effect that plays a significant role in the stabilization of the secondary structure. They determined that the addition of each glycine unit systematically contributes to the stabilization energy that is defined as the energy gained from the addition of the mth Gly unit to Gly_{m-1} relative to the energy gained from the formation of Gly_3 from Gly_2 and that this effect has an effective radius of about 10 glycine units. This is a suitable problem to reinvestigate as a model application of MP2 and scaled MP2 methods, with two purposes. The first purpose is to examine the MP2-level energies to see to what extent long-range correlation effects contribute to the stabilization (since dispersion effects are neglected in functionals like B3LYP). The second purpose is to present systematic timings for the implementations described in the previous section, as a function of the chain length.

To study the long-range correlation effects, we redefine the stabilization energy as δE_m, the increment in energy gained by the addition of the mth glycine unit to Gly_{m-1} relative to addition of $(m\text{-}1)^{\text{th}}$ glycine unit to Gly_{m-2}; that is $\delta E_m = \Delta E_m - \Delta E_{m-1}$where $\Delta E_m = E_m - E_{m-1}$and E_m is the energy of Gly_m. We have investigated this system by calculating the energy increments at the HF, RI-MP2, SOS-MP2, and MOS-MP2 levels of theory using the Dunning cc-pVXZ (X = D, T) basis and the corresponding auxiliary basis optimized for RI-MP2 calculations.[43] The optimized geometries of the Gly_m were taken from Horvath et al.[42] Two-point extrapolation was carried out to evaluate δE_m at CBS for RI-MP2, MOS-MP2, and SOS-MP2. B3LYP results (cc-pVTZ) are also included for purposes of comparison. The δE_m is a direct quantitative measure of the energy gained due to the cooperative long-range effects and it decays with increasing length of the glycine chain. Figure 8 clearly reflects this idea and also indicates that correlation effects

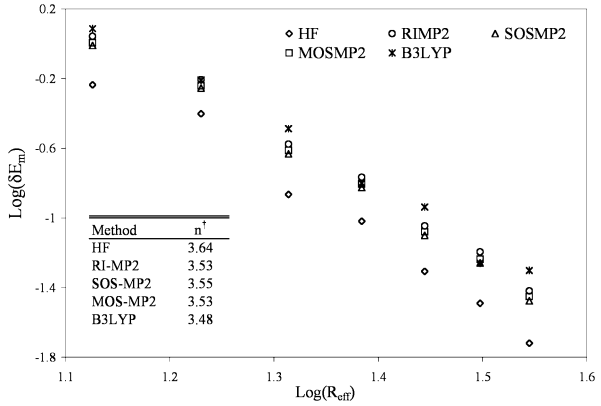

Figure 9. Log plot of decay of stabilization energy of Gly_m with length of the glycine chain. The cc-pVTZ basis set was used for HF and B3LYP calculations. The extrapolated results at CBS are shown for RI-MP2, SOS-MP2, and MOS-MP2. (†) δE_m ($\propto 1/R_{\text{eff}}^n$) where n is the slope of the best fit line for each method.

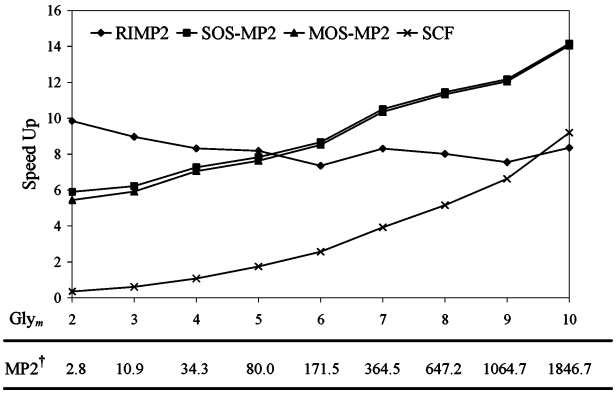

Figure 10. Speed-ups obtained relative to conventional MP2 (given by the ratio of CPU timings of regular MP2 and indicated method) for glycine chains (Gly_m, $m = 2-10$) performed on IBM Power 3 p640 server (375 MHz) using cc-pVDZ basis. (†) Conventional MP2 CPU timing (in minutes) for Gly_m.

strongly influence δE_m as can be observed by comparing the results of Hartree−Fock and various flavors of MP2. A decay plot of δE_m ($\propto 1/R_{\text{eff}}^n$) with the effective length of Gly_m, defined as the distance between the N and C termini, would highlight the nature of interactions that are responsible for the stabilization of the oligoglycine with increasing chain length. Figure 9 is a plot of $\log(|\delta E_m|)$ vs $\log(R_{\text{eff}})$ for the various methods accompanied by a table indicating the corresponding slopes obtained for each method. The predicted "n"-distance dependence by the various methods lies between 3.5 and 3.6. This indicates that the long-range cooperative interactions are primarily due to electrostatic dipole−dipole interactions assisted by the internal hydrogen bonding and to a certain extent due to dipole−induced dipole-type interactions leading to a slightly faster decay than the expected ($1/R^3$) behavior. The similarity in the decay behavior predicted by the various MP2 methods and DFT (B3LYP) indicates that dispersion-type effects are not important for the stabilization of this system and it is also hard to conclude if the quality of MP2-type results is superior to DFT (B3LYP) results or vice-versa. Among the MP2-level methods, MOS-MP2 seems to slightly improve the SOS-MP2 description to closely mimic RI-MP2-type behavior.

Figure 10 shows the overall speed-ups of RI-MP2, SOS-MP2, and MOS-MP2 relative to conventional MP2 for the glycine systems, where speed-up is defined as the ratio of CPU timing of regular MP2 to CPU timing of the method under consideration. The cc-pVDZ basis and the corresponding auxiliary basis

was used for all these calculations and were carried out on IBM Power 3 p640 servers (375 MHz) with a memory limit of 1 GB. As per the discussion on computational cost in the previous section, we can see that the speed-ups obtained by SOS-MP2 and MOS-MP2 are very similar because the cost of the dominating step, namely, formation of the **X** matrix, in both cases is roughly the same. MOS-MP2 speed-ups are slightly lower than SOS-MP2 due to the extra cost incurred from the formation of the "modified" two- and three-center integrals as discussed in the previous section. This extra cost is very small in comparison to the total CPU time. MOS-MP2 is about 5−14 times faster than the regular MP2. RI-MP2 is faster than SOS-MP2 and MOS-MP2 for smaller Gly_n ($n = 2-5$). This is a result of a contest between the costs of forming the **X** matrix for each quadrature point in eq 14 for SOS-MP2 and MOS-MP2 vs the fifth-order formation of $(ia|jb)$ in RI-MP2. Eventually, the overhead of repeating calculations in the Laplace-RI formalism becomes smaller than the fifth-order step in the conventional RI-MP2 method as the system size increases, resulting in crossovers around roughly 400 basis functions for glycine chains. The significance of the fourth-order scaling algorithm is evident while comparing the SCF CPU times to the various flavors of MP2 in Figure 10. The RI-MP2 energy evaluation becomes more expensive than the SCF for systems with about 35−40 first row elements while this is not the case with SOS-MP2 and MOS-MP2.

V. Conclusions

1. In this paper, we have suggested an alternative scaling of the opposite-spin (OS) component of the MP2 correlation energy as a workaround to the strongly damped long-range description of our scaled opposite-spin (SOS)-MP2 method.[21] This involves the introduction of "modified" two-electron integrals that are a linear combination of the regular Coulomb repulsion integrals and integrals with the long-range operator, $\mathrm{erf}(\omega\mathbf{r})/\mathbf{r}$, in the MP2 energy expression for the OS component. The long-range integrals serve as an inter-electronic distance dependent correcting factor that would help compensate for the absence of the same-spin (SS) component and also give the full MP2 correlation at the long-range limit, by construction. We call this scheme modified opposite-spin (MOS)-MP2 that depends on a single parameter (ω).

2. By performing a range of chemical tests largely involving covalent compounds, we established that the parameter ω could be tuned to improve the MP2 results for a particular property. For instance, MOS-MP2 showed statistical improvements relative to conventional MP2 energies in barrier height estimations that were more favorable than SCS-MP2 and SOS-MP2, whose results, obtained with the recommended scaling factors, were in fact degraded. Also, $\omega = 0.6$ au appears to be a favorable value for MOS-MP2 that provides improved MP2 results over a range of tested properties and remains comparable to the quality of the SCS-MP2 and SOS-MP2 results.

3. As expected, the interaction potential energy curves computed for a few weakly interacting dimers showed that the scaled MP2 methods consistently underestimate the binding energy relative to MP2. This can appear to improve the MP2 quality provided MP2 overestimates the energy relative to higher correlation methods like CCSD(T). MOS-MP2 was found to certainly improve the SOS-MP2 description. The extent of improvement is limited by an interesting observation that the contribution of the SS component can be slightly greater than the OS contribution to the MP2 dimer binding energy (at intermediate distances), thereby, making it impossible for MOS-MP2, irrespective of the ω parameter value, to compensate for the missing SS component.

4. The MOS-MP2 energy can also be evaluated with a modified fourth order scaling algorithm similar to the previously described SOS-MP2 formalism that involves a Laplace transformation of the energy denominator and use of the resolution-of-the-identity (RI) approximation, at almost no extra cost.

5.The usefulness of MOS-MP2, both accuracy and computational, was illustrated by the study of long-range interactions in polyglycines. It was shown that the stabilization energies decay roughly as $R_{\mathrm{eff}}^{-3.5}$ with the effective length of the glycine chain as a result of the cooperative dipole−dipole interactions aided by hydrogen-bonding and possibly, some dipole−induced dipole-type interactions as well. The MOS-MP2 method exhibits here that it is possible to retain the accuracy of MP2 or RI-MP2 method (especially while computing relative energies) with the correct physical description of long-range correlation and at the same time, obtain computational efficiency (without exploiting localization!). It thus seems a very suitable substitute for our SOS-MP2 formalism and a great starting point for lower scaling MP2 methods.

Acknowledgment. This work was supported in part by funding from Q-Chem Inc. via an SBIR subcontract from the National Institutes of Health, and in part by the Department of Energy through the Computational Nanosciences program. M.H.G. is a part owner of Q-Chem Inc.

References and Notes

(1) Møller, C.; Plesset, M. S. *Phys. Rev.* **1934**, *46*, 618.
(2) Szabo, A.; Ostlund, N. S. *Modern Quantum Chemistry: Introduction to Advanced Electronic Structure Theory*; Dover Publications: New York, 1996.
(3) Parr, R. G.; Yang, W. *Density-functional theory of atoms and molecules*; Oxford: New York, 1989.
(4) Mourik, T. V.; Wilson, A. K.; Dunning, T. H. *Mol. Phys.* **1999**, *96*, 529.
(5) Kristyan, S.; Pulay, P. *Chem. Phys. Lett.* **1994**, *229*, 175.
(6) Helgaker, T.; Klopper, W.; Koch, H.; Noga, J. *J. Chem. Phys.* **1997**, *106*, 9639.
(7) Byrd, E. F. C.; Sherrill, C. D.; Head-Gordon, M. *J. Phys. Chem. A* **2001**, *105*, 9736.
(8) Baker, J.; Pulay, P. *J. Comput. Chem.* **2002**, *23*, 359.
(9) Saebo, S.; Pulay, P. *Annu. Rev. Phys. Chem.* **1993**, *44*, 213.
(10) Schutz, M.; Hetzer, G.; Werner, H. J. *J. Chem. Phys.* **1999**, *111*, 5691.
(11) Werner, H. J.; Manby, F. R.; Knowles, P. J. *J. Chem. Phys.* **2003**, *118*, 8149.
(12) Lee, M. S.; Maslen, P. E.; Head-Gordon, M. *J. Chem. Phys.* **2000**, *112*, 3592.
(13) Ayala, P. Y.; Kudin, K. N.; Scuseria, G. E. *J. Chem. Phys.* **2001**, *115*, 9698.
(14) Ayala, P. Y.; Scuseria, G. E. *J. Chem. Phys.* **1999**, *110*, 3660.
(15) Feyereisen, M.; Fitzgerald, G.; Komornicki, A. *Chem. Phys. Lett.* **1993**, *208*, 359.
(16) Weigend, F.; Haser, M.; Patzelt, H.; Ahlrichs, R. *Chem. Phys. Lett.* **1998**, *294*, 143.
(17) Grimme, S. *J. Chem. Phys.* **2003**, *118*, 9095.
(18) Gerenkamp, M.; Grimme, S. *Chem. Phys. Lett.* **2004**, *392*, 229.
(19) Grimme, S. *J. Comput. Chem.* **2003**, *24*, 1529.
(20) Piacenza, M.; Grimme, S. *J. Comput. Chem.* **2004**, *25*, 83.
(21) Jung, Y. S.; Lochan, R. C.; Dutoi, A. D.; Head-Gordon, M. *J. Chem. Phys.* **2004**, *121*, 9793.
(22) Sinnokrot, M. O.; Sherrill, C. D. *J. Phys. Chem. A* **2004**, *108*, 10200.
(23) Dombroski, J. P.; Taylor, S. W.; Gill, P. M. W. *J. Phys. Chem.* **1996**, *100*, 6272.
(24) Hetzer, G.; Schutz, M.; Stoll, H. *J. Chem. Phys.* **2000**, *113*, 9443.
(25) Kong, J.; White, C. A.; Krylov, A. I.; Sherrill, C. D.; Adamson, R. D.; Furlani, T. R.; Lee, M. S.; Lee, A. M.; Gwaltney, S. R.; Adams, T. R.; Ochsenfeld, C.; Gilbert, A. T. B.; Kedziora, G. S.; Rassolov, V. A.; Maurice, D. R.; Nair, N.; Shao, Y.; Besley, N. A.; Maslen, P. E.; Dombroski, J. P.; Daschel, H.; Zhang, W.; Korambath, P. P.; Baker, J.; Byrd, E. F. C.; Voorhis, T. V.; Oumi, M.; Hirata, S.; Hsu, C. P.; Ishikawa, N.; Florian, J.; Warshel,

A.; Johnson, B. G.; Gill, P. M. W.; Head-Gordon, M.; Pople, J. A. *J. Comput. Chem.* **2000**, *21*, 1532.

(26) Head-Gordon, M. *Mol. Phys.* **1999**, *96*, 673.

(27) Pople, J. A.; Head-Gordon, M.; Raghavachari, K. *J. Chem. Phys.* **1987**, *87*, 5968.

(28) Kendall, R. A.; Dunning, T. H., Jr.; Harris, R. J. *J. Chem. Phys.* **1992**, *96*, 6796.

(29) Curtiss, L. A.; Raghavachari, K.; Redfern, P. C.; Pople, J. A. *J. Chem. Phys.* **1997**, *106*, 1063.

(30) Curtiss, L. A.; Raghavachari, K.; Trucks, G. W.; Pople, J. A. *J. Chem. Phys.* **1991**, *94*, 7221.

(31) Zhao, Y.; Lynch, B. J.; Truhlar, D. G. *J. Phys. Chem. A* **2004**, *108*, 2715.

(32) Dunning Jr., T. H. *J. Chem. Phys.* **1989**, *90*, 1007.

(33) Halkier, A.; Helgaker, T.; Jørgensen, P.; Klopper, W.; Koch, H.; Oslen, J.; Wilson, A. K. *Chem. Phys. Lett.* **1998**, *286*, 243.

(34) Cybulski, S. M.; Toczylowski, R. R. *J. Chem. Phys.* **1999**, *111*, 10520.

(35) Purvis, G. D.; Bartlett, R. J. *J. Chem. Phys.* **1982**, *76*, 1910.

(36) Halkier, A.; Koch, H.; Jørgensen, P.; Christiansen, O.; Nielsen, I. M. B.; Helgaker, T. *Theor. Chem. Acc.* **1997**, *97*, 150.

(37) Goldman, N.; Fellers, R. S.; Brown, M. G.; Braly, L. B.; Keoshian, C. J.; Leforestier, C.; Saykally, R. J. *J. Chem. Phys.* **2002**, *116*, 10148.

(38) Almlöf, J. *Chem. Phys. Lett.* **1991**, *181*, 319.

(39) Eichkorn, K.; Treutler, O.; Öhm, H.; Häser, M.; Ahlrichs, R. *Chem. Phys. Lett.* **1995**, *240*, 283.

(40) Jung, Y.; Sodt, A.; Gill, P. M. W.; Head-Gordon, M. *Proc. Natl. Acad. Sci. U.S.A.* **2005**, *102*, 6692.

(41) Dunlap, B. I. *Phys. Chem. Chem. Phys.* **2002**, *2*, 2113.

(42) Horvath, V.; Varga, Z.; Kovacs, A. *J. Phys. Chem. A* **2004**, *108*, 6869.

(43) Weigend, F.; Kohn, A.; Hattig, C. *J. Chem. Phys.* **2002**, *116*, 3175.

(44) Ogilvie, J. F.; Wang, F. Y. *J. Mol. Struct.* **1992**, *273*, 277.